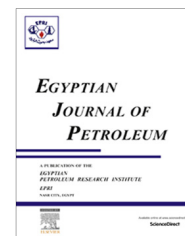




Egyptian Petroleum Research Institute  
Egyptian Journal of Petroleum

[www.elsevier.com/locate/egyjp](http://www.elsevier.com/locate/egyjp)  
[www.sciencedirect.com](http://www.sciencedirect.com)



FULL LENGTH ARTICLE

# Estimation of the non records logs from existing logs using artificial neural networks



Mehdi Mohammad Salehi<sup>a,\*</sup>, Mehdi Rahmati<sup>b</sup>, Masoud Karimnezhad<sup>c</sup>,  
Pouria Omidvar<sup>d</sup>

<sup>a</sup> Sahand University of Technology, Tabriz, Iran

<sup>b</sup> Petroleum University of Technology, Ahwaz, Iran

<sup>c</sup> Researcher at National Iranian South Oil Company, Ahwaz, Iran

<sup>d</sup> Exploration Directorate Company, Tehran, Iran

Received 4 September 2016; revised 4 November 2016; accepted 10 November 2016

Available online 30 November 2016

## KEYWORDS

Well logging;  
Petrophysics;  
Neural network;  
Wire-line logs;  
Geophysical

**Abstract** Finding the information of the hydrocarbon reservoirs from well logs is one of the main objectives of the engineers. But, missing the log records (due to many reasons such as broken instruments, unsuitable borehole and etc.) is a major challenge to achieve it. Prediction of the density and resistivity logs ( $R_t$ , DT and LLS) from the conventional wire-line logs in one of the Iranian south-west oil fields is the main purpose of this study. Multilayer neural network was applied to develop an intelligent predictive model for prediction of the logs. A total of 3000 data sets from 3 wells (A, B and C) of the studied field were used. Among them, the data of A, B and C wells were used to constructing and testing the model, respectively. To evaluate the performance of the model, the mean square error (MSE) and correlation coefficient ( $R^2$ ) in the test data were calculated. A comparison between the MSE of the proposed model and recently intelligent models shows that the proposed model is more accurate than others. Acceptable accuracy and using conventional well logging data are the highlight advantages of the proposed intelligent model.

© 2016 Egyptian Petroleum Research Institute. Production and hosting by Elsevier B.V. This is an open access article under the CC BY-NC-ND license (<http://creativecommons.org/licenses/by-nc-nd/4.0/>).

## 1. Introduction

Density and resistivity are two important parameters in reservoir evaluation and geophysical/geomechanical studies. Hence, the ultimate objective of reservoir evaluation studies by density

and resistivity in the petroleum industry is to economically establish the existence of producible hydrocarbon reservoirs. Also, geophysical/geomechanical studies by using density and resistivity can be used to determine hydrocarbons presence, determination of fluid type-gas, oil, water, bitumen, computation of porosity, computation of water saturation and lithology [1,2]. These parameters could be determined from either laboratory methods or well logging operation. The laboratory methods are very expensive and time consuming. Since 1980s, geophysical well logging has been one of the key tools in hydrocarbon resource evaluation and management alike. Well

\* Corresponding author.

E-mail addresses: [mehdi.salehi83@gmail.com](mailto:mehdi.salehi83@gmail.com) (M.M. Salehi), [mehdi\\_mr3@yahoo.com](mailto:mehdi_mr3@yahoo.com) (M. Rahmati), [masoud\\_karimnezhad@yahoo.com](mailto:masoud_karimnezhad@yahoo.com) (M. Karimnezhad), [pouriaomidvar@yahoo.com](mailto:pouriaomidvar@yahoo.com) (P. Omidvar).

Peer review under responsibility of Egyptian Petroleum Research Institute.

<https://doi.org/10.1016/j.ejpe.2016.11.002>

1110-0621 © 2016 Egyptian Petroleum Research Institute. Production and hosting by Elsevier B.V.

This is an open access article under the CC BY-NC-ND license (<http://creativecommons.org/licenses/by-nc-nd/4.0/>).

logging is also considered as an integral part of formation evaluation that can provide great amount of data, which can be the best candidate to help in stages in developing reservoir static and dynamic models for efficient production and economic recovery [1]. But, it is quite common for the log records to be missing due to many reasons such as broken instruments, hole conditions, instrument failure, or loss of data due to inappropriate storage and incomplete logging [3,4]. This can result in the absence of some logging intervals or even an entire log type. Therefore, it is appeared that finding a new method for estimation of these parameters is necessary. For this purpose, many studies have been focused on prediction of the wire-line logs. Most of these studies have been tried to propose an intelligent model using artificial intelligence (AI) techniques. The artificial intelligence techniques have the remarkable ability to establish a complicated mapping between non-linearly linked input and output data [5].

In recent years, there has been an increasing interest in developing artificial neural network models for prediction of the density and resistivity logs from conventional wire-line logs in the world. A review of the published related studies is presented here.

In 2012, Masoudi et al. used Bayesian Network in identifying effective logs, i.e. feature selection for determining productive zones through oil wells. Due to the results, the ratio of Latero log Deep Resistivity (LLD) to Latero log Shallow Resistivity (LLS) and individually LLD are the most effective raw features for detecting productive zones through oil wells. Based on the results of the latter, porosity and water saturation are the most important extracted features for evaluating productive zones [6].

Bahrpeyma et al., [7] proposed a new fast fuzzy modelling method (FFMM) using Ink Drop Spread (IDS) and Center of Gravity (COG) operators to estimate missing log of density. For performance evaluation of the proposed model, they also estimated the density log using artificial neural network (ANN) and conventional fuzzy logic (FL). To predict the Sonic log (DT), density log (RHOB) and photoelectric log (PEF) and neutron log (NPHI) were used as input. Their results indicate that the accuracy of the proposed method is almost the same as the accuracy of ANN and TS-FIS (Takagi-Sugeno fuzzy inference system) methods but computational complexity, storage requirements and simplicity of the proposed method are much better.

Bahrpeyma et al., [8] employed active learning method (ALM) to estimate another missing log in hydrocarbon reservoirs, namely the density log. The regression and normalized mean squared error for estimating density log using ALM were equal to 0.9 and 0.042, respectively. The results, including errors and regression coefficients, proved that ALM was successful in processing the density estimation.

In this paper, by using artificial neural networks, it is tried to propose an intelligent predictive model to predict the density and resistivity wire-line logs from another conventional wire-line logs ( $R_{xo}$ ,  $S_w$ ,  $S_{xo}$ , NPHI, RHOB,  $R_{xo}$ , LLD, MSFL) in Mansouri oil field which is one of the most important Iranian southwest oil fields. Some advantages of this study include the following:

- The estimation technique is relatively simple, economical and quick.

- Inputs (depth, compressional wave velocity and density data) are available in most wells.
- Generally, well logs can provide a continuous record over the entire well; thus, using well log data as input can be estimated over whole of the well.
- In the ranges of the used data, the proposed model is intelligent.

## 2. Methodology

In this study, artificial neural networks (ANNs), which is one of the all techniques, was applied to develop an intelligent predictive model for prediction of the logs. ANNs, firstly introduced by McCulloch and Pitts [9], is a mathematical model of biological events in order to imitate the capability of biological neural structures with the purpose of designing an intelligent information processing system. An adaptive neural network is a network structure consisting of large number of elemental units, called neurons, organized in input, hidden, and output layers. Any neuron in the network is characterized by some features such as input weights, a threshold, and an activation function. The adjusting weights connect the neurons in different layers, so that a particular input, according to a learning algorithm, leads to a specific target output [9,10]. Neural networks can solve problems which cannot be solved by means of common calculations and discover highly complex relationships between several variables. A neural network works as a learning process from provided information, trains the data to form certain patterns for each subject, then predicts targets with the output model. In petroleum engineering, these networks are used when there is not enough data for interpretation [11,12].

Multi Layer Perceptron (MLP) network is one the common ANNs that may consist of one or more hidden layers and the input of each hidden or output layer is an inner product of the outputs of a previous layer and weights (Fig. 1). Each layer is composed of nodes and in the fully connected networks considered in this paper each node connects to every node in subsequent layers. In addition, the activation function of hidden layer(s) in MLPs is logistic sigmoid or hyperbolic tangent function that produces output  $[0, 1]$  and  $[-1, 1]$ , respectively [13,14].

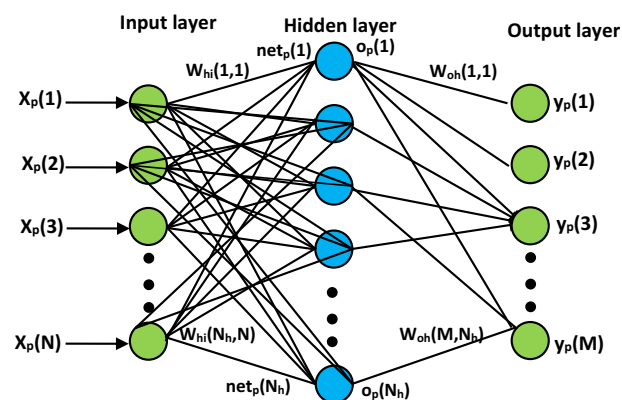


Figure 1 Architecture of MLP.

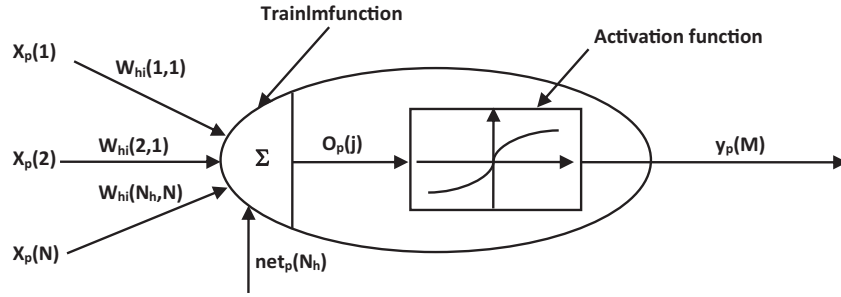


Figure 2 Mathematical representation of a neural cell in the network.

The input layer distributes the inputs to subsequent layers. Input nodes have linear activation functions and no thresholds. Each hidden unit node and each output node have thresholds associated with them in addition to the weights. The hidden unit nodes have nonlinear activation functions and the outputs have linear activation functions. Hence, each signal feeding into a node in a subsequent layer has the original input multiplied by a weight with a threshold added and then is passed through an activation function that may be linear or nonlinear (hidden units). Only three layer MLPs will be considered in this paper since these networks have been shown to approximate any continuous function. For the actual three-layer MLP, all of the inputs are also connected directly to all of the outputs. The training data consists of a set of  $N_v$  training patterns  $(x_p, t_p)$  where  $p$  represents the pattern number. In Fig. 1,  $x_p$  corresponds to the  $N$ -dimensional input vector of the  $p$ th training pattern and  $y_p$  corresponds to the  $M$ -dimensional output vector from the trained network for the  $p$ th pattern. For ease of notation and analysis, thresholds on hidden units and output units are handled by assigning the value of one to an augmented vector component denoted by  $x_p(N+1)$ . The output and input units have linear activations. The input to the  $j$ th hidden unit,  $net_p(j)$ , is expressed by:

$$net_p(j) = \sum_{k=1}^{N+1} w_{hi}(j, k) \cdot x_p(k) \quad 1 \leq j \leq N_h \quad (1)$$

With the output activation for the  $p$ th training pattern,  $O_p(j)$ , being expressed by:

$$O_p(j) = f(net_p(j)) \quad (2)$$

The nonlinear activation is typically chosen to be the sigmoidal function:

$$f(net_p(j)) = \frac{1}{1 + e^{-net_p(j)}} \quad (3)$$

In (1) and (2), the  $N$  input units are represented by the index  $k$  and  $w_{hi}(j, k)$  denotes the weights connecting the  $k$ th input unit to the  $j$ th hidden unit.

The overall performance of the MLP is measured by the mean square error (MSE) expressed by:

$$E = \frac{1}{N_v} \sum_{p=1}^{N_v} E_p = \frac{1}{N_v} \sum_{p=1}^{N_v} \sum_{i=1}^M [t_p(i) - y_p(i)]^2 \quad (4)$$

where

$$E_p = \sum_{i=1}^M [t_p(i) - y_p(i)]^2$$

$E_p$  corresponds to the error for the  $p$ th pattern and  $t_p$  is the desired output for the  $p$ th pattern. This also allows the calculation of the mapping error for the  $i$ th output unit to be expressed by:

$$E_i = \frac{1}{N_v} \sum_{p=1}^{N_v} [t_p(i) - y_p(i)]^2 \quad (5)$$

with the  $i$ th output for the  $p$ th training pattern being expressed by:

$$y_p(i) = \sum_{k=1}^{N+1} w_{oi}(i, k) \cdot x_p(k) + \sum_{j=1}^{N_h} w_{oh}(i, j) \cdot O_p(j) \quad (6)$$

In (6),  $w_{oi}(i, k)$  represents the weights from the input nodes to the output nodes and  $w_{oh}(i, j)$  represents the weights from the hidden nodes to the output nodes [15,16]. Fig. 2 is a mathematical model of a neural cell in which the combined function, the transfer function, weight of each input, and bias are illustrated.

### 3. Data acquisition and available data

This study is conducted on the data derived from the Mansouri Oil Field on the South-West of Iran. This field which has a very complicated geology is located on the North-East of Ahvaz city, adjacent to Yaran oilfields and contains one the biggest fracture oil reservoirs in the world. The oil field mentioned is 39 km in length and 5.3 km in width and has a closure about 2143 m and water oil contact about 2272 m. Its capacity of production is 100,000 bbl/day from Aghajari formation and initial bubble reservoir pressure is above the point pressure and net pay zone is about 129 m.

Lithology of this field is very variable and consists largely of dolomite, anhydrite, sandstone, shale but it can be claimed that the main lithology is carbonate rock.

According to available wire line logs data such as neutron porosity (NPHT), bulk density (RHOB), shallow resistivity (LLS), deep resistivity (LLD), corrected Gamma ray (GR), the production zone (Aghajari formation) divided to 8 pays. The main lithology of pay one is limestone and dolomite and pays two to five are include sandstone. The 6th pay consists of dolomite, sandstone and shale and 7th pay establish limestone, sandstone, dolomite and shale. The last pay has been made limestone and shale.

In this study three well logs are selected for interpretation by resistivity-based regression estimation which are as following:  $R_t$ , LLS and DT. For this purpose, three wells A, B and C related pay one has been chosen.

**Table 1** Range of used for designing of the models.

Parameter	Range	Mean
	Training data	Training data
Dt	47.9303–79.1499	61.8734
LLD	5.6990–537.6521	114.7395
LLS	4.1572–289.4127	165.8320
Rt	5.7780–453.5643	223.8205
Rxo	0.3743–51.3674	5.8207
Sw	0.0002–1	0.2364
Sxo	0.0055–1	0.6383
RHOB	2.1386–2.7030	2.5299
MSFL	0.3667–51.7816	5.8101

In order to estimation of the non records logs from existing logs using artificial neural networks, 1000 data were used for development of the ANN models. Initially, 700 data were employed for training of ANN model, and 150 data for testing of it were utilized randomly. Data of train and test sets were applied for determination of optimum architecture of the model. The performance dataset, which contains 150 data, was used for evaluation of the model performance after determination of the model with optimum architecture. Range of the used data for designing of the models is presented in Table 1. Normalization of data is a method that causes increasing of ANN performance. One of the common approaches for normalization of data is performed by mean and standard deviation (STD) of data using Eq. (7). Based on this approach, input and output parameters are normalized so that they will have zero mean and one standard deviation:

$$X'_i = \frac{X_i - \mu_i}{\sigma_i} \quad (7)$$

where  $X_i$  is current value of the parameter,  $X'_i$  is normalized value of the current value,  $\mu_i$  and  $\sigma_i$  are mean and standard deviation values of the current value, respectively. For evaluation of the models in train, test, and performance stages, total average absolute deviation (TAAD) was performed, which is defined as:

$$\text{TAAD}(\%) = \frac{100}{N} \sum \frac{|\text{LOG}_{\text{Measured}} - \text{LOG}_{\text{Predicted}}|}{\text{LOG}_{\text{Measured}}} \quad (8)$$

where  $N$  is total number of data in each data set,  $\text{LOG}_{\text{Measured}}$  is measured permeability ratio, and  $\text{LOG}_{\text{Predicted}}$  is predicted permeability ratio by the model.

#### 4. Development of models

In this paper, multilayer perception network has been used. mean square error (MSE) has been chosen as the operating function for the training data. As the LM algorithm error decreases faster than that of other algorithms, Levenberg–Marquardt network with Trainlm function has been used to train the network.

The data obtained from well logging of A and B wells were used for designing and training of the network. The designed network was tested on well C in order to investigate its efficacy. Training data are used to determine weights. Although, validation data are used during training, they play no direct role in data weighting. The task of validation data is to mon-

itor the generalization ability of network in parallel with its training. After all training data were presented to the network in a complete cycle, the validation data were entered to the network by using obtained weights and the values are calculated. The errors of training and validation data were re-calculated after each complete cycle of presenting training data to the network. As it can be seen, after a tolerance stage, data validation error firstly decreased and after a while increased. It means that the network gradually loses its generalization and tries to keep training data without being able to recognize proper relationship between input and output data. Therefore, the training process should be stopped, when network produces more validation errors after a series of consecutive times and weights related to the least validation error should be considered as the best result of training process. If the level of errors is not optimal, a new round of training should be started. After the errors of training and validation data are reached to the desired level, the test data which are not used until this stage, used to final measuring of network's generalization ability. These data are entered to the trained network (which its optimal weight coefficients have been determined) and its output is calculated and compared with the original values. If the obtained error (training data error) be in an optimal level, the work is completed. Now it is possible to utilize from trained network in estimating of diagrams in wells which lack the desired diagram.

In the present study, the input patterns (i.e. raw interpretation of well log) were divided into three sets of training, experimental and test sets in order to train the designed network. In this way, 70% of data were randomly allocated to training and rests of them were considered as experimental and testing data. The reason for considering such high percentage of data to network training was that the network can perceive the dominant patterns of inputs and outputs and be able to adapt itself with different conditions. In this approach, designed network will be trained by training data sets. Additionally, the network will be tested during the training process by testing data sets; as a result, optimized training of network is assessed by choosing proper repeats. The test data sets are usually utilized for evaluating estimates of network about intended parameter and this set of data do not have any functionality in the processes of training and testing the network. Factors considered in this study are as follow:

##### 4.1. Log $R_t$

$R_{xo}$ ,  $Sw$ ,  $Sxo$  are inputs in designing the first network. Data of  $R_t$  are used as favourable outputs for training the network. Data of wells A and B are used in order to design the network and its training as well. The final programming is carried out by Matlab. When using this software, firstly, input and output matrices are applied to the network as training set. Data are processed prior to training the network for more efficiency of the network. The initial value of network variables is selected randomly in a small interval. Next, the network is trained by training data as soon as these programs run and final adjusted variables will be in our hand. Optimized numbers of middle neurons are obtained by trial and error. It means we start with few numbers of middle neurons. Then, their number increases until the least error is acquired. Thus, for the first state, the network used is composed of 4 sub layers.



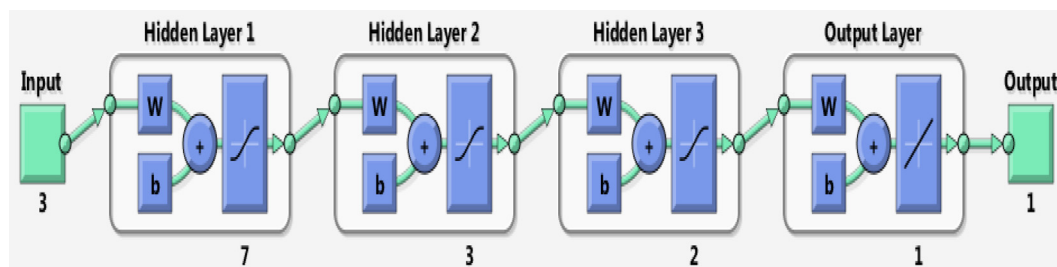


Figure 3 The perception network for the first state.

Input layer, as it was mentioned, includes  $R_{xo}$ ,  $S_w$ ,  $S_{xo}$ . The first sub layer has three neurons, the second one has 3 neurons, and the third sub layer has also 2 neurons. Output layer includes a neuron as well. TANSIG transform function is used for the first, second, and third sub layers and PURELIN function is used for output layer. Fig. 3 depicts the perception network for the first state.

The convergence of error during the network training depends upon the number of example used for training the network. If the number of patterns and/or the number of middle layer neuron is low, the network cannot learn the existing relation between inputs and outputs. Moreover, if the number of middle layer neurons is more than necessary level, the network starts to preserve the patterns so that they act properly for training but they are not good for training and are not able to be generalized. As it was mentioned before, the performance function for training data set is the mean square error. Levenberg-Marquardt network with *Trainlm* function is used for training the network because of the fact that the error of LM algorithm reduces more rapidly than other existing algorithms.

#### 4.2. Log DT

In the second network,  $R_{xo}$ ,  $R_{HOB}$  and  $N_{PHI}$  are inputs data and  $DT$  is used as favourable outputs. In this case, the network used is composed of 4 sub layers. Input layer, as it was mentioned, includes  $R_{xo}$ ,  $R_{HOB}$  and  $N_{PHI}$ . The first sub layer has 8 neurons, the second one has 5 neurons, and the third sub layer has also 4 neurons. Output layer includes a neuron as well. TANSIG transform function is used for the first, second, and third sub layers and PURELIN function is used for output layer. Fig. 4 shows the perception network for the second case.

#### 4.3. Log LLS

In the last item,  $LLD$  and  $MSFL$  are inputs data and  $LLS$  is used as outputs. In this case, the network used is composed of 3 sub layers. The first sub layer has 7 neurons, the second one has 5 neurons, and output layer includes a neuron as well. TANSIG transform function is used for the first, second, and output layer. Fig. 5 shows the perception network for the third state.

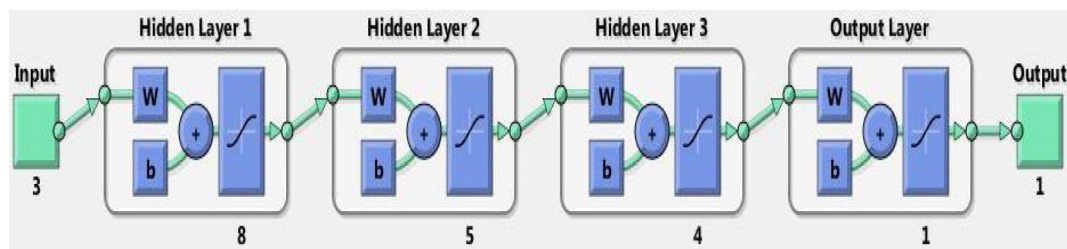


Figure 4 The perception network for the second state.

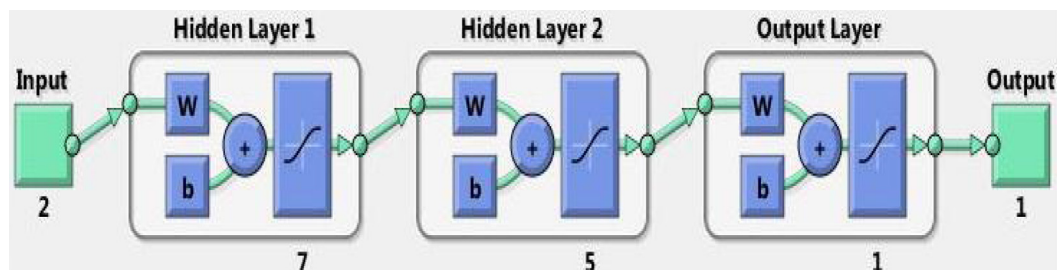
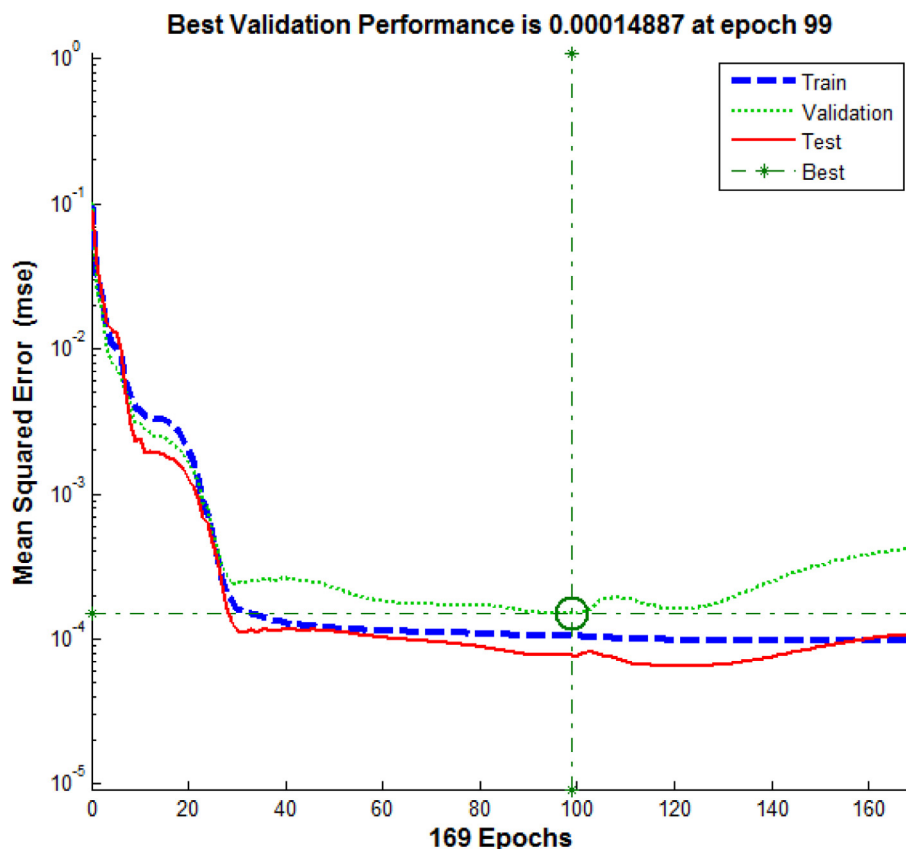


Figure 5 The perception network for the third state.



**Figure 6** The mean square error curve versus the number of repetitions performed in the training mode, validation and test for the first case.

## 5. Result and discussion

### 5.1. Estimation of $\log R_t$

If the diagrams of  $R_{xo}$ ,  $S_w$ ,  $S_{xo}$  are used as network inputs (state 1), mean square error of training data is equal to

0.0001 and mean square error of validation data is nearly 0.00015 and mean square error of the test data is equal to 0.00009, and the changes of mean square error against the number of repetitions are shown in Fig. 6.

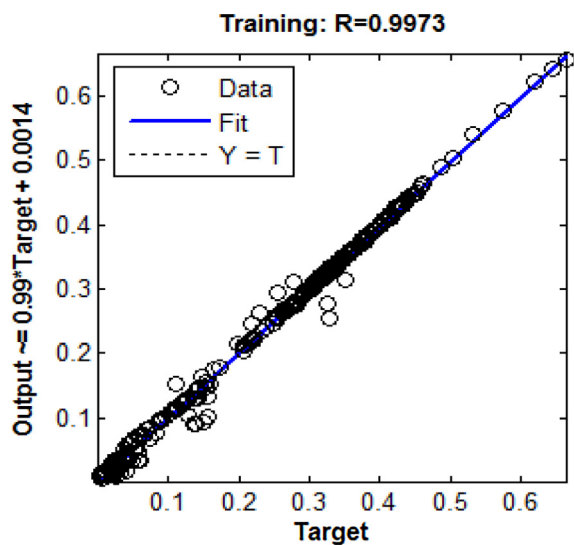


**Figure 7** The correlation coefficient (R) between network and measured  $R_t$  for training data.

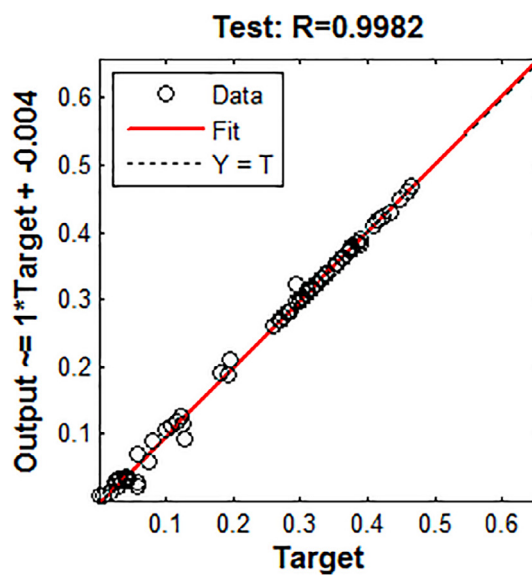


**Figure 8** The correlation coefficient (R) between network and measured  $R_t$  for test data.

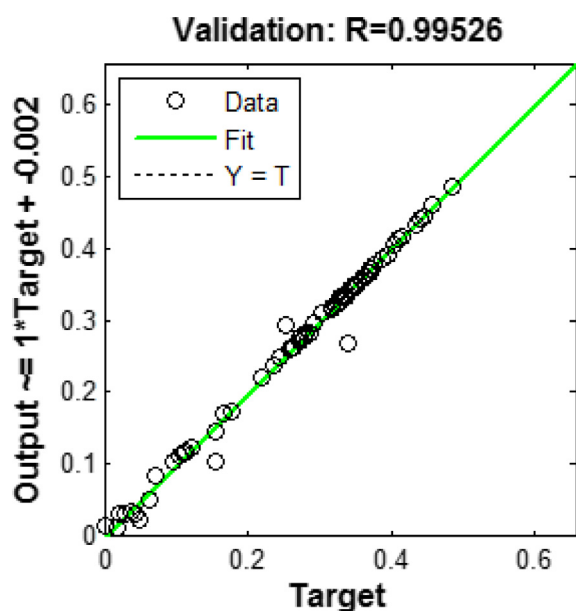


**Figure 9** The correlation coefficient (R) between network and measured  $R_t$  for validation data.

The correlation coefficient of training, test, validation and total data are 0.9973, 0.9982, 0.9953 and 0.9972, respectively. Figs. 7–10 represent the correlation coefficient (R) between

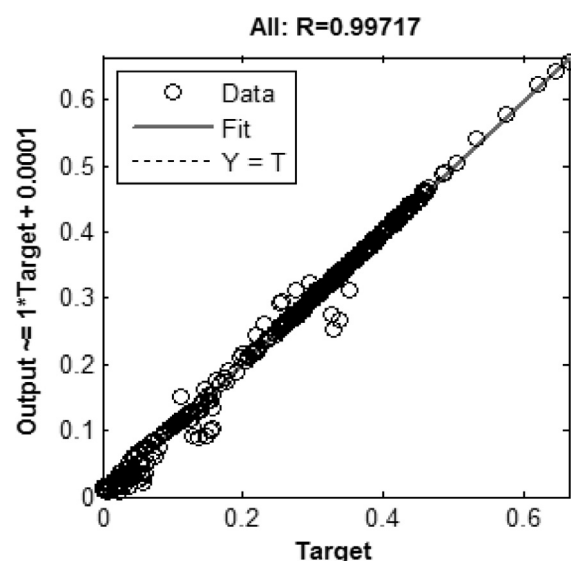


**Figure 10** The correlation coefficient (R) between network and measured  $R_t$  for total data.

network and measured  $R_t$  for training, test, validation and total network, respectively.

Fig. 11 shows the predicted data network related to wells C. The data that have been indicated with a small circle indicates

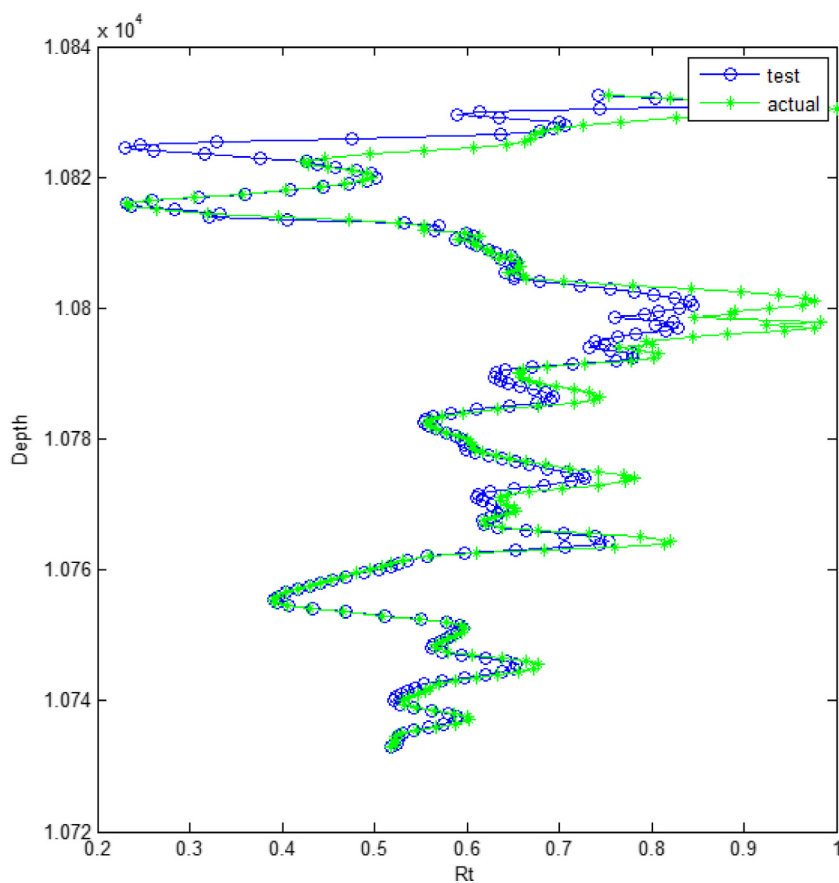


**Figure 11** Comparison between real well log data and predicted data by the neural network for  $R_t$  in the well C.

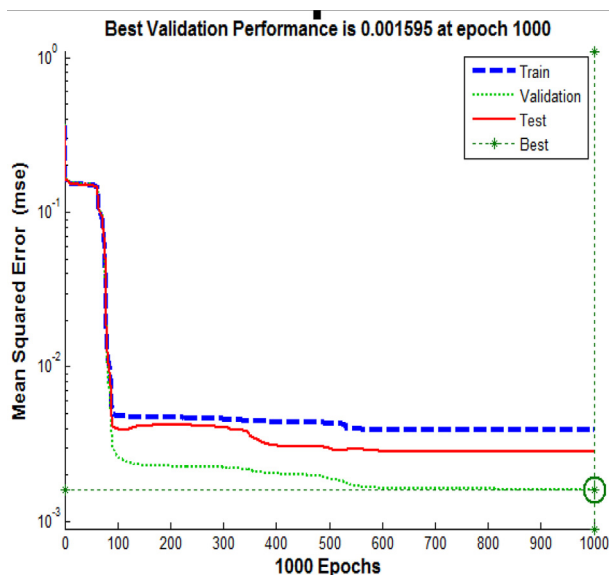


**Figure 12** The mean square error curve versus the number of repetitions performed in the training mode, validation and test for the second state.

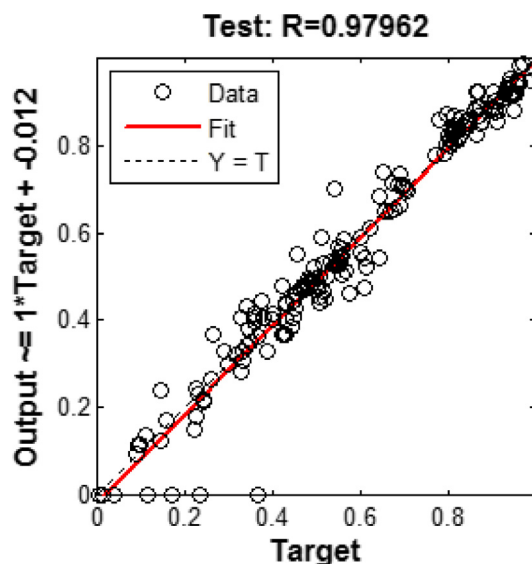


**Figure 14** correlation coefficient (R) between DT network and measured DT for test data.

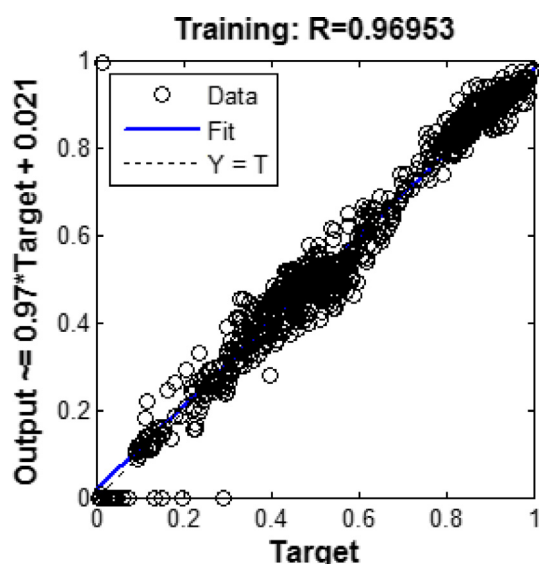


**Figure 13** The correlation coefficient (R) between DT network and measured DT for training data.

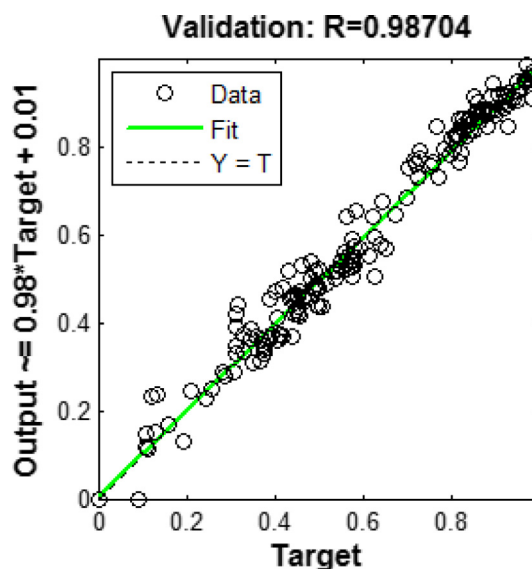


**Figure 15** correlation coefficient (R) between DT network and measured DT for validation data.

Rtreal data logging and data that are indicated with an asterisk, indicating predictive neural network designed for the first case. Obviously, there are a strong relation between these variables as the high value of  $R^2$  (0.878) supports our proposed approach.

In the neural network which is designed in the first state, anticipation of Rt diagram behaviour is addressed. By selecting appropriate input ( $R_{xo}$ ,  $S_w$ ,  $S_{xo}$ ), the anticipation is appropriately performed. Generally, the investigated depths of measured diagrams and fabricated diagrams by neural network have good agreement; except in the depths near to 10,800 feet which a little deviation from the main diagram is observed.

High correlation coefficient and low error rate demonstrates a strong network for the intended goal. This network shows that for obtaining Rt diagram, having  $S_{xo}$ ,  $S_w$ ,  $R_{xo}$  diagrams and designed neural network are sufficient in field and if measured Rt diagram is flawed, we can consider anticipate its behaviour using this network and auxiliary diagrams.

## 5.2. Estimation of log DT

In this case, the mean square error of training data is equal to 0.004, the mean square error of validation and test data are 0.0016 and 0.0035, respectively. Fig. 12 illustrates the mean



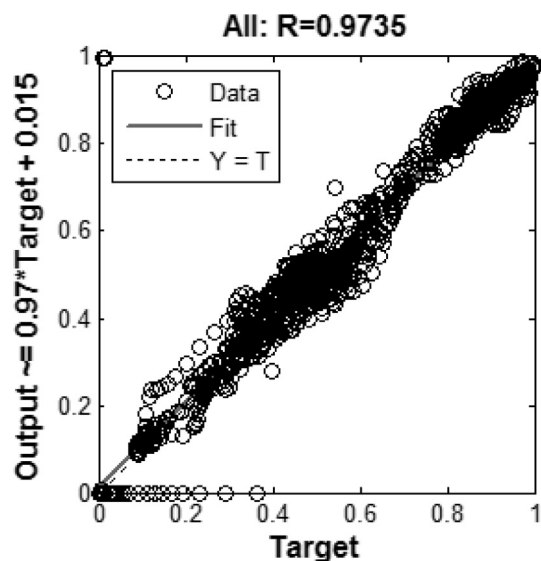


**Figure 16** correlation coefficient (R) between DT network and measured DT for total data.

square error versus the number of repetitions for training, validation and test data in the second case.

For this case, the correlation coefficient of training, test, validation and total data are 0.9695, 0.9796, 0.9870 and 0.9735, respectively. Figs. 13–16 show the correlation coefficient (R) between DT network and measured DT for training, test, validation and total network, respectively in the men-

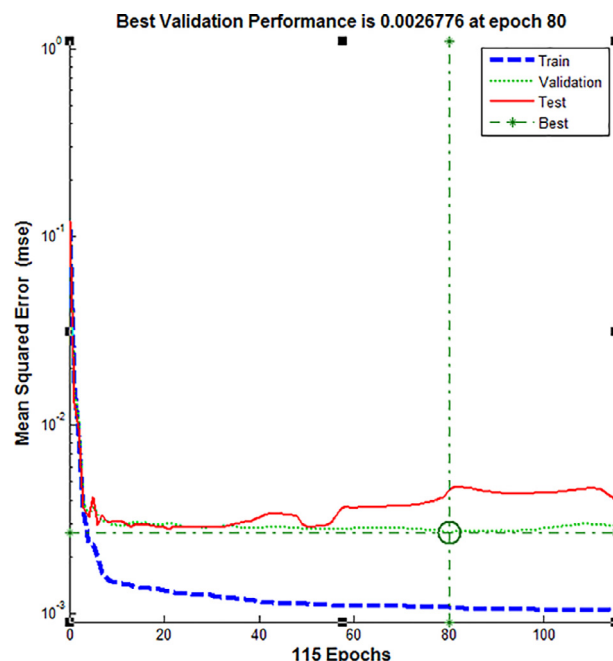


**Figure 18** The mean square error curve versus the number of repetitions performed in the training mode, validation and test for the third state.

tioned case. Also, Fig. 17 shows the predicted data network related to wells C.

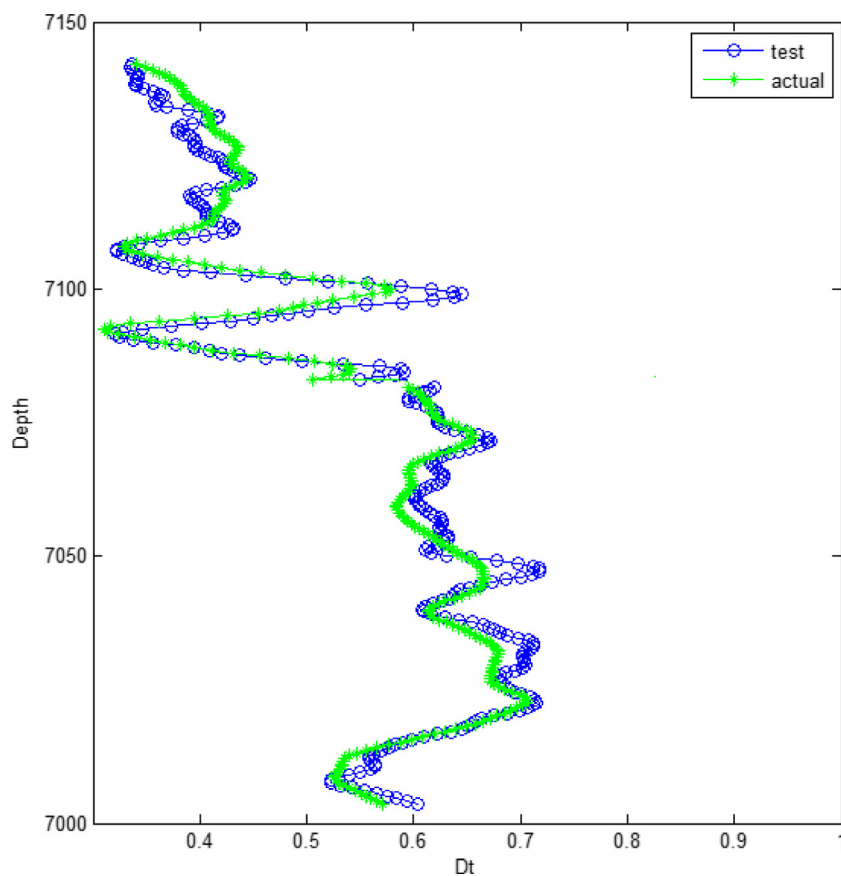


**Figure 17** Comparison between real well log data and predicted data by the neural network for DT in the well C.

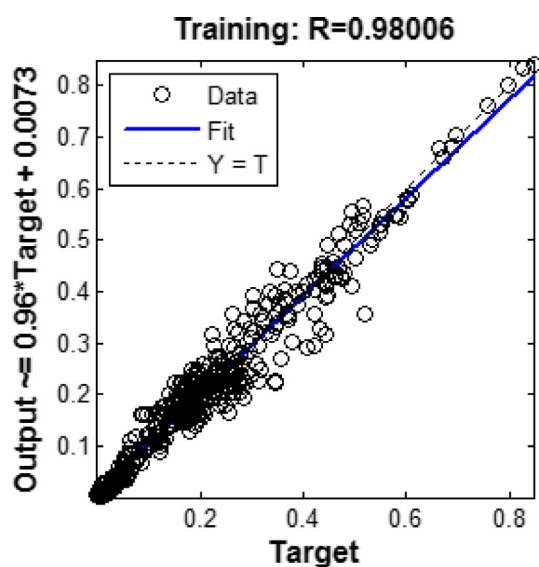


**Figure 19** The correlation coefficient (R) between LLS network and measured LLS for training data.

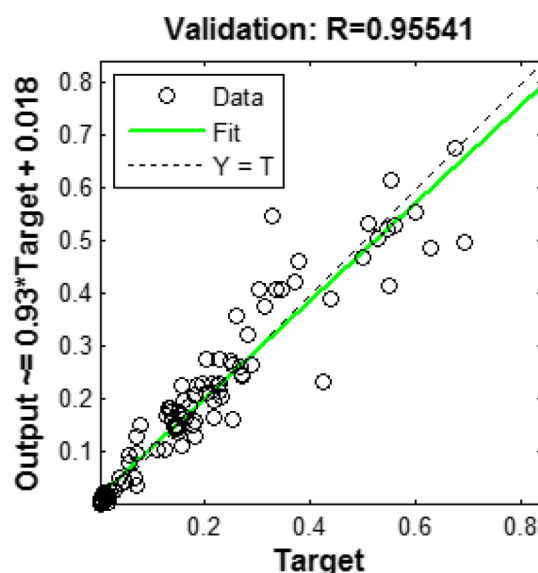


**Figure 21** correlation coefficient (R) between LLS network and measured LLS for validation data.

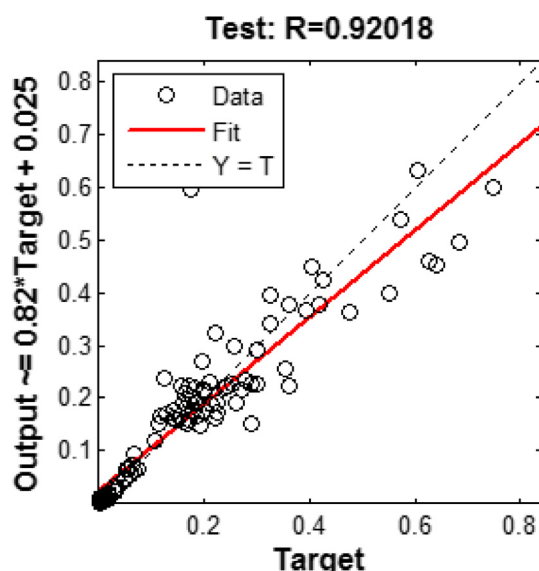


**Figure 20** The correlation coefficient (R) between LLS network and measured LLS for test data.

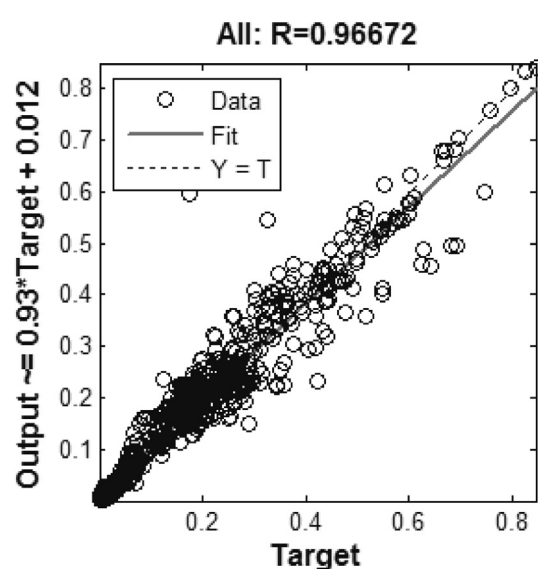


**Figure 22** The correlation coefficient (R) between LLS network and measured LLS for total data.

In the neural network which is designed in the second state, the anticipation of DT diagram behaviour is addressed. By selecting appropriate inputs (NPHI, RHOB, R<sub>xo</sub>), the anticipation is appropriately accomplished. Though, the made diagram by neural network is not adapted in some points on the measured diagram, but general state and the process of diagram is not appropriately anticipated. It is worth noting that the value of mean square error represents network negligible error.

High correlation coefficient and low error rate demonstrates a strong network for the intended goal. This network shows that for obtaining DT diagram, having NPHI, RHOB, RXO diagrams and designed neural network are sufficient in

the field and if measured Rt diagram is flawed, we can consider anticipating its behaviour using this network and auxiliary diagrams.

### 5.3. Estimation of log LLS

In the third case, the mean square error of training, validation and test data are equal to 0.001, 0.0027 and 0.004, respectively. Fig. 18 shows the changes of mean square error against the number of repetitions.

In the third state, the correlation coefficient of training, test, validation and total data are 0.9801, 0.9202, 0.9554 and 0.9667, respectively. Figs. 19–22 show the correlation coefficient (R) between LLS network and measured LLS for train-

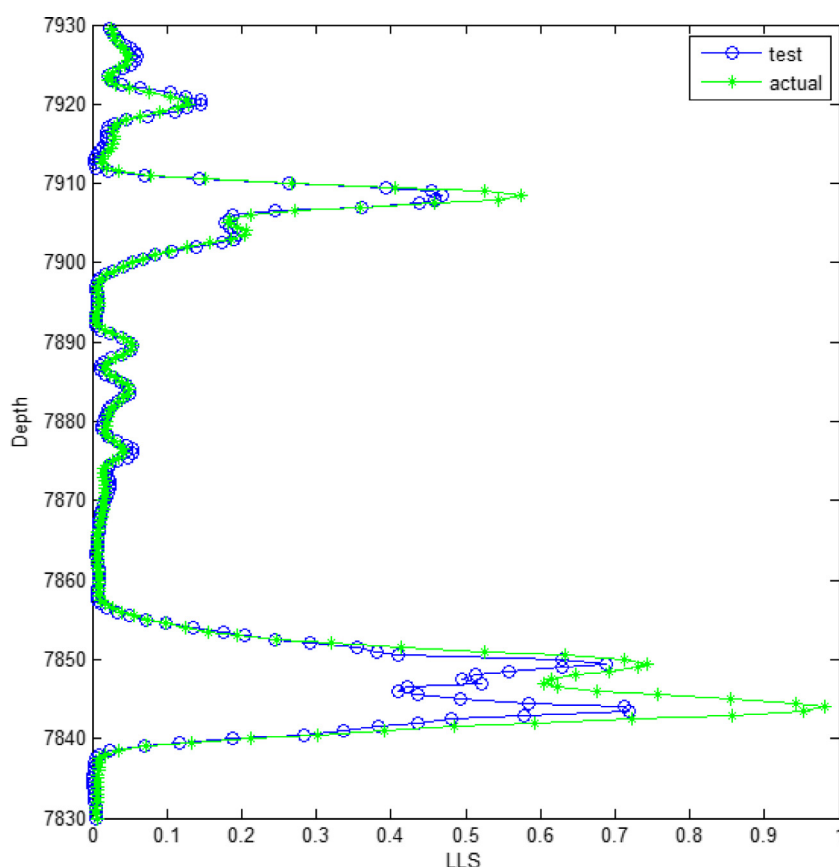


**Figure 23** Comparison between real well log data and predicted data by the neural network for LLS in the well C.

ing, test, validation and total network, respectively in the mentioned case. Also, Fig. 23 shows the predicted data network related to wells C.

In the neural network, which is designed in the third state, the anticipation of LLS diagram behaviour is addressed. By selecting appropriate inputs (MSFL, LLD), anticipation has been appropriately implemented. However, as it is clear from the figure, the made diagram by neural network is not completely adapted in some depths around 7840–7850, but it has an acceptable anticipation in this range.

High correlation coefficient and low error rate demonstrates a strong network for the intended goal. This network shows that for obtaining LLS diagram, having MSFL, LLD diagrams and the designed neural network are sufficient in the field and if measured LLS diagram is flawed, we can consider anticipating its behaviour using this network and auxiliary diagrams.

## 6. Conclusion

In this research, three networks with multilayer error back-propagation algorithm and Levenberg-Marquardt algorithm have been used by MATLAB software for estimating diagrams. The results from the networks are:

Artificial networks with error back-propagation algorithm after necessary training are able to find governing non-linear relations on different diagrams of well and to implement anticipating intended diagrams and/or their recovering by

estimating such relations. In addition, these networks don't need the awareness of primary mathematical model to understand the relation between input variables and output function; and output function sensitivity to input variables can be investigated only by primary studies, and they can be used in the modelling.

A multi-layer perceptions network with error back-propagation algorithm by getting required training, can anticipate Rt, DT and LLS diagrams with adequate precision which is an important diagrams in the evaluation of hydrocarbon reservoirs. This issue can be investigated from the test results and extending the designed network for anticipating C well diagrams that had no intervention in network training. By comparing the estimated diagrams of network was measured for this well by real diagram and in addition, correlation coefficient shows high ability and accuracy of the designed artificial neural networks for anticipating such diagrams in the intended wells. Hence, they can be used for oil field wells of Ahvaz that lack the intended diagrams.

Generally, modelling error in the first network is about 1.22% for anticipating Rt diagram, it is about 4.00% in the second network for anticipating Dt diagram and it is about 5.17% in the third network for anticipating LLS diagram.

## References

- [1] A. Timur, *Advances in well logging*, J. Petrol. Technol. 34 (06) (1982) 1–181.

- [2] M.R.J. Wyllie, M.B. Spangler, Application of electrical resistivity measurements to problems of fluid flow in porous media, *Am. Assoc. Petrol. Geol. (AAPG) Bull.* (1952).
- [3] M.R. Rezaee, J.K. Applegate, Shear velocity prediction from wire line logs, an example from Carnarvon Basin, NW Shelf, Australia, SEG (Society of Exploration Geophysicists) Expanded Abstracts (16 (RP1)) (1997) 945–947.
- [4] M. Rajabi, B. Bohloli, E. Ahangar, Intelligent approaches for prediction of compressional, shear and Stoneley wave velocities from conventional well log data: a case study from the Sarvak carbonate reservoir in the Abadan Plain (South-western Iran), *J. Comput. Geosci.* 36 (2010) 647–664.
- [5] P. Nakutnyy, K. Asghari, A. Torn, Analysis of water flooding through application of neural networks, in: Canadian International Petroleum Conference, Calgary, Alberta, June 17–19, 2008.
- [6] P. Masoudi, F. Hourfar, A. Mazaheri Torei, An improvement in estimating petrophysical parameters by utilizing normalizing mapping on inputs of artificial neural networks, in: 8th Iranian Student Mining Engineering Conference. Tehran, Iran, pp 1–8, 2011.
- [7] F. Bahrpeyma, B. Golchin, C. Cranganu, Fast fuzzy modelling method to estimate missing logs in hydrocarbon reservoirs, *J. Petrol. Sci. Eng.* 112 (2013) 310–321.
- [8] F. Bahrpeyma, C. Cranganu, B. Zamani Dadaneh, Active learning method for estimating missing logs in hydrocarbon reservoirs, *J. Artif. Intell. Approaches Petrol. Geosci.* (2015) 209–224.
- [9] W.S. McCulloch, W. Pitts, A logical calculus of the ideas imminent in nervous activity, *Bull. Math. Biophys.* 5 (1943) 115–133.
- [10] L.V. Fausett, *Fundamentals of Neural Networks: Architectures, Algorithms and Applications*, first ed., Pearson publication, India, 1993.
- [11] G. Auda, M.S. Kamel, Modular neural networks a survey, *Int. J. Neural Syst.* 9 (2) (1999) 129–151.
- [12] L.F. Ayala, T. Ertekin, Analysis of gas-cycling performance in gas/condensate reservoirs using neuro-simulation, in: SPE Paper 95655, SPE Annual Technical Conference and Exhibition, Dallas, TX, October 9–12, pp. 1–10, 2005.
- [13] D. Kaviani, T.D. Bui, J.L. Jensen, C.L. Hanks, The application of artificial neural networks with small data sets: an example for analysis of fracture spacing in the Lisburne Formation, North-eastern Alaska, *SPE Reserv. Eval. Eng.* (June 2008) 598–605.
- [14] H. Demuth, M. Beale, M. Hagan, *Neural Network Toolbox 5 User's Guide*, The Math Works Inc., Natick, MA, 2007. A.A. Elgibaly, A.M. Elkamel, A new correlation for predicting hydrate formation conditions for various gas mixtures and inhibitors. *Fluid Phase Equilib.* 152 (1998) 23–42.
- [15] G. Cybenko, Approximation by superposition of a sigmoidal function, *Math. Control Signals Syst.* 2 (4) (1989) 303–314.
- [16] W.H. Delashmit, M.T. Manry, Recent developments in multilayer perceptron neural networks, in: Proceedings of the 7th Annual Memphis Area Engineering and Science Conference MAESC, 2005.